

GSA Data Repository 2011032

Supplementary materials for:

Termination of back-arc spreading: zircon dating of a giant oceanic core complex

Kenichiro Tani¹, Daniel J. Dunkley², Yasuhiko Ohara^{3, 1}

¹Institute for Research on Earth Evolution, Japan Agency for Marine-Earth Science and Technology, Yokosuka, 237-0061, Japan

²National Institute of Polar Research, Tokyo, 190-8518, Japan

³Hydrographic and Oceanographic Department of Japan, Tokyo, 104-0045, Japan

Sample preparation and analytical procedures.

Tani et al. Figure DR1

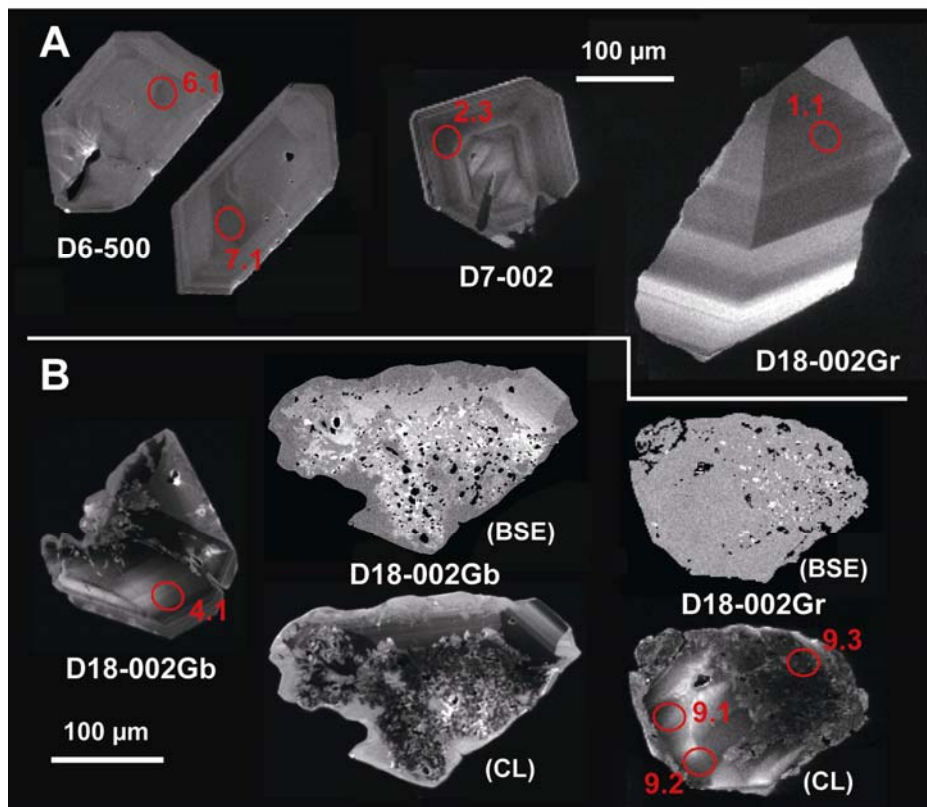


Figure DR1. Representative cathodoluminescence (CL) and backscattered electron (BSE) images of Godzilla Megamullion zircons analyzed by SHRIMP. Areas of spot analyses are marked with red ellipses, and labeled according to grain number and spot number, as listed in Table DR1. (A) Zircon crystals and

fragments with euhedral morphologies and oscillatory to sector-type internal zoning, typical of magmatic growth. (B) Zircon crystals with margins and patches modified by coupled dissolution-reprecipitation. CL image of grain 4 from gabbroic sample D18-002Gb shows alteration of low CL, high U-Th magmatic zircon which grades towards the margins to uniformly high-CL, inclusion-poor modified zircon. Unanalyzed grain from the same sample shows alteration of low CL, high U-Th magmatic zircon to inclusion-rich high CL zircon, which grades towards the margins to uniformly high-CL, inclusion-poor zircon. Dark patches in the BSE image include porosity; bright inclusions are Th, U and/or Y-rich minerals such as xenotime and thorite. Similar texture is observed in a grain 9 from feldspathic vein D18-002Gr.

Tani et al. Figure DR2

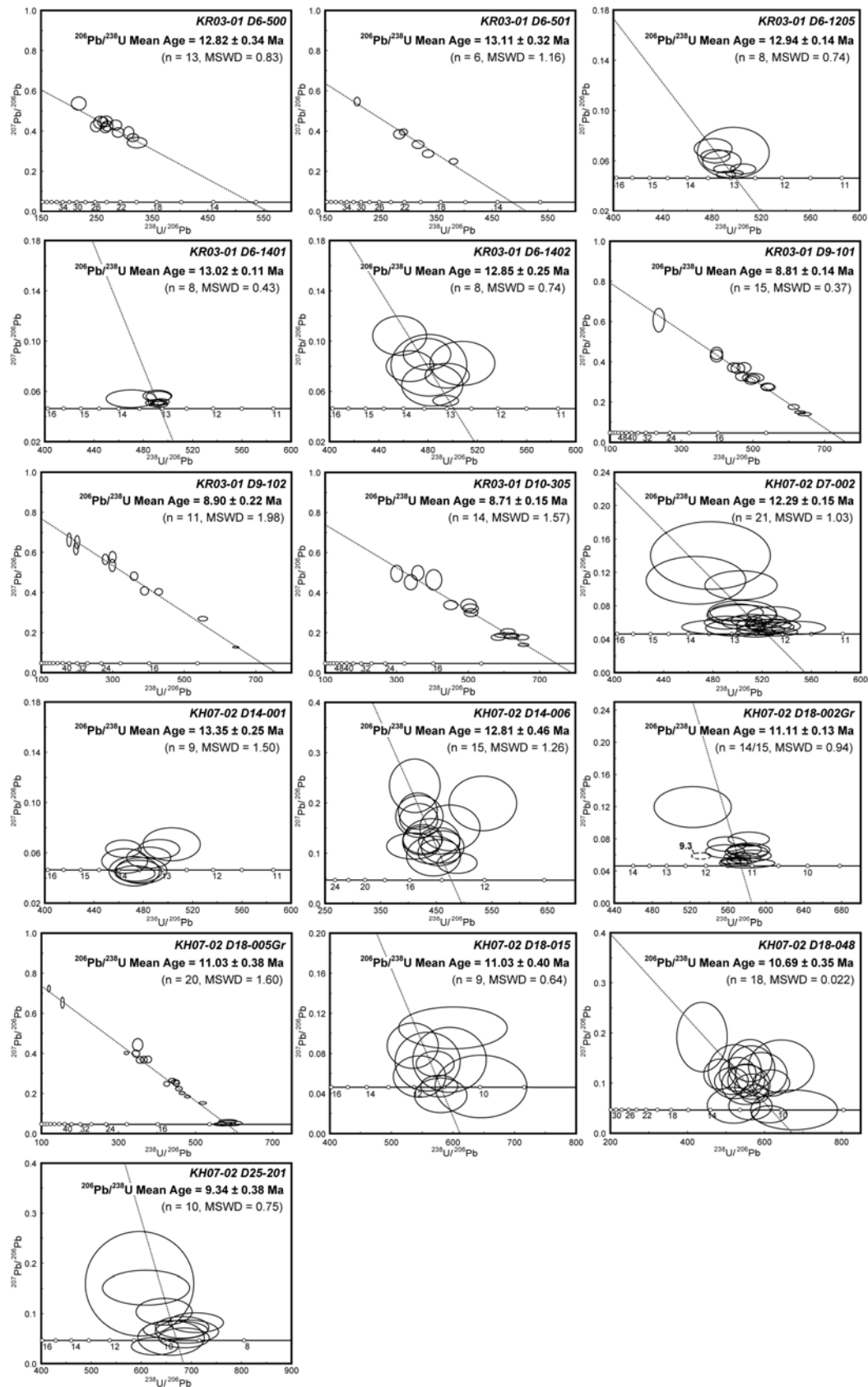


Figure DR2. ^{230}Th -corrected Tera-Wasserburg concordia plots of SHRIMP-analyzed samples. Error ellipses represent 68.3 % confidence levels (approximately one standard deviation). Quoted ages are weighted means of ^{207}Pb and ^{230}Th corrected $^{206}\text{Pb}/^{238}\text{U}$ spot ages (n analyses, errors at 95% confidence intervals). Solid ellipse: analysis used in weighted mean age calculation; dotted ellipse: analysis excluded. Labels on individual ellipses correspond to analysis spot numbers in Table DR1. Dashed lines represent linear projections from weighted mean ages to common lead compositions estimated using the two-stage common-Pb model of Stacey and Kramers (1975).

Tani et al. Figure DR3



Figure DR3. Cut surface of sample D18-002. An undeformed feldspathic vein (D18-002Gr) intrudes into the mylonitized gabbroic host (D18-002Gb). Hydrothermal alteration is present in both rock types, giving plagioclase grains a milky appearance.

SAMPLE PREPARATION AND ANALYTICAL PROCEDURES

Sample preparation

The zircons were separated from fresh hand specimens by coarse crushing (to ~300 µm) in a tungsten-carbide rotary mill. For small samples (<200 g), original rock fragments were hand-crushed in a tungsten-carbide mortar. The heavy minerals were concentrated by panning and further processed with a hand magnet, and the resultant fractions were purified using heavy liquid (diiodomethane) separation. Zircon grains were then handpicked under a stereo microscope. The grains are ~50 to several hundred µm long, with variable grain shapes with dominant forms ranging from prisms to dipyramids in both gabbroic and leucocratic samples.

Zircon U-Pb analyses

Zircon U-Pb ages were analyzed over several sessions using the Sensitive High-Resolution Ion Microprobe (SHRIMP)-II at the National Institute of Polar Research (NIPR), Japan. The zircon grains were mounted in epoxy, polished down to grain centers, cleaned and then coated with ~10 nm of high-purity gold. Backscattered electron and cathodoluminescence (CL) images were obtained using the JEOL JSM7300 scanning electron microprobe at NIPR to visualize internal zoning. A primary O₂⁻ ion beam with a surface current ranging from -14 to -5 nA between sessions was used to produce 30 × 25 to 25 × 20 µm flat-floored oval craters. Abundance of U was calibrated against zircon standard SL13 (238 ppm), provided by Australian National University. Reduction of raw data for standards and samples was performed using the SQUID v.1.12a (Ludwig 2001), and Isoplot v.3.71 (Ludwig 2003) add-ins for Microsoft Excel 2003. Sample U-Pb measurements were calibrated against zircon standard TEMORA-2 (417 Ma; Black et al., 2004) using a calibration exponent of 2. Scatter on ²⁰⁴Pb-corrected (Pb/U)/(UO/U²) ratios of TEMORA-2 in each sessions was typically less than 1 % (2σ), with external spot-to-spot errors of less than 2 % (2σ); the latter errors are included in the errors of weighted mean ages for each sample/session. Weighted mean ages of samples for which data was obtained during multiple sessions were calculated from the weighted mean ages of data for each session. Zircon isotopic compositions and ages are listed in Table DR1. Initial ²³⁸U-²³⁰Th disequilibrium was corrected using the method described in Parrish and Noble (2003). The Th/U ratio of the magma at the time of zircon crystallization, required for disequilibrium correction, was assumed as (Th/U)_{magma} = 3.42 ± 0.85 (2SD, n = 6), as estimated from whole-rock analyses of basaltic rocks collected from the Godzilla

Megamullion (unpublished data of O. Ishizuka). Corrections for common Pb on U/Pb values and ages for samples were performed using the ^{207}Pb -correction method described in Ireland and Williams (2003), which assumes concordance between $^{206}\text{Pb}/^{238}\text{U}$ and $^{207}\text{Pb}/^{235}\text{U}$ ages. For most sessions, the Stacey & Kramers (1975) common Pb model for the approximate age of each analysis was used. However, in some sessions (samples D6-500, D6-501, D9-101, D9-102, D10-305 and D18-005Gr sessions 1 and 2), a high proportion of surface common Pb was measured, which was derived from contamination by Pb-bearing samples with an approximate age of 550Ma. In these cases, a Stacey & Kramers (1975) common Pb model age of 550Ma was used, and the appropriateness of the model age was checked against the corrected age of an in-house zircon standard in the same grain mount. Ages reported in the main text and figures are weighted means of $^{207}\text{Pb}-^{230}\text{Th}$ -corrected $^{206}\text{Pb}/^{238}\text{U}$ ages, quoted at the 95 % confidence level, from 6 – 21 analyses per sample (Table DR1). Data from spots partially or completely overlapping domains of altered zircon, as assessed from CL images, were excluded from mean age calculations of magmatic zircon.

REFERENCES CITED

- Black, L. P., Kamo, S. L., Allen, C. M., Davis, D. W., Aleinikoff, J. N., Valley, J. W., Mundil, R., Campbell, I. H., Korscha, I. J., Williams, I. S. and Foudoulis, C., (2004). Improved $^{206}\text{Pb}/^{238}\text{U}$ microprobe geochronology by the monitoring of a trace-element-related matrix effect; SHRIMP, ID-TIMS, ELA-ICP-MS and oxygen isotope documentation for a series of zircon standards: Chemical Geology, v. 205, p. 115-140. doi: 10.1016/j.chemgeo.2004.01.003.
- Harigane, Y., Michibayashi, K., and Ohara, Y., 2008, Shearing within lower crust during progressive retrogression: Structural analysis of gabbroic rocks from the Godzilla Mullion, an oceanic core complex in the Parece Vela backarc basin: Tectonophysics, v. 457, p. 183-196, doi: 10.1016/j.tecto.2008.06.009.
- Ireland, T.R., and Williams, I.S., 2003, Considerations in zircon geochronology by SIMS, in Hanchar, J.M., Hoskin, P.W.O., eds., Zircon, Reviews in Mineralogy & Geochemistry, Volume 53: Washington D.C., Mineralogical Society of America, p. 215-241.
- Ludwig, K.R., 2001, SQUID: A user's manual: Berkeley Geochronology Center, Special Publication 2, 22 p.
- Ludwig, K.R., 2003, User's manual for isoplot 3.00: A geochronological toolkit for Microsoft Excel: Berkeley Geochronology Center, Special Publication 4, 71 p.
- Parrish, R.R., and Noble, N.R., 2003, Zircon U-Th-Pb geochronology by isotope dilution - Thermal ionization mass spectrometry (ID-TIMS), in Hanchar, J.M., Hoskin,

P.W.O., eds., Zircon, Reviews in Mineralogy & Geochemistry, Volume 53:
Washington D.C., Mineralogical Society of America, p. 182-213.

Stacey, J.C., and Kramers, J., 1975, Approximation of terrestrial lead isotope evolution by
a two-stage model: Earth and Planetary Science Letters, v. 26, p. 207–221.

Table DR1. SHRIMP zircon U-Pb analyses of the Godzilla Megamullion rocks.

Spot	$^{206}\text{Pb}_c$ (%)	U (ppm)	Th (ppm)	$^{232}\text{Th}/^{238}\text{U}$	$^{238}\text{U}/^{206}\text{Pb}$	$\pm\%$	$^{207}\text{Pb}/^{206}\text{Pb}$	$\pm\%$	$^{206}\text{Pb}^*$ (ppm)	$^{206}\text{Pb}/^{238}\text{U}$ age (Ma) (1)	1 sigma err	$^{206}\text{Pb}/^{238}\text{U}$ Mean age (Ma) (1) (95%)	MSWD	$^{238}\text{Pb}/^{206}\text{U}$ (Thc)	$\pm\%$	$^{207}\text{Pb}/^{206}\text{Pb}$ (Thc)	$\pm\%$	$^{206}\text{Pb}/^{238}\text{U}$ age (Ma) (Thc)	1 sigma err	Note	$^{206}\text{Pb}/^{238}\text{U}$ Mean age (Ma) (Thc) (95%)	MSWD				
KR03-01 D6-500 (gabbro, stderr = 0.13 %)																								12.82±0.34	0.83	
D6-500-1.1	36	145	153	1.09	323.0	3.6	0.342	5.1	0.386	12.82	0.63	(n = 13)													(n = 13)	
D6-500-2.1	42	155	132	0.88	308.3	2.0	0.391	5.2	0.432	12.19	0.57														sec	
D6-500-3.1	48	66	41	0.64	256.9	3.1	0.443	4.6	0.222	13.03	0.74														sec	
D6-500-4.1	46	111	93	0.87	284.7	2.5	0.430	3.8	0.334	12.12	0.54														sec	
D6-500-5.1	46	95	74	0.80	269.5	2.4	0.425	3.9	0.304	12.94	0.58														sec	
D6-500-6.1	49	99	77	0.80	267.5	2.7	0.449	3.8	0.319	12.37	0.60														sec	
D6-500-7.1	39	152	121	0.82	316.1	2.1	0.367	3.6	0.412	12.48	0.42														sec	
D6-500-8.1	42	110	89	0.84	289.1	2.4	0.393	4.0	0.326	12.95	0.53														sec	
D6-500-9.1	45	109	96	0.91	265.8	2.3	0.416	3.9	0.351	13.39	0.58														sec	
D6-500-10.1	46	84	62	0.77	248.7	2.6	0.424	4.3	0.288	14.06	0.69														sec	
D6-500-11.1	48	111	101	0.94	261.0	2.3	0.445	3.6	0.366	12.79	0.56														sec	
D6-500-12.1	59	68	46	0.70	217.6	4.0	0.537	4.0	0.270	12.04	0.92														sec	
KR03-01 D6-501 (gabbro, stderr = 0.13 %)																									13.11±0.32	1.16
D6-501-1.1	35	150	154	1.06	317.6	2.2	0.333	3.9	0.406	13.26	0.43	(n = 6)														(n = 6)
D6-501-2.1	29	197	124	0.65	336.0	2.0	0.287	4.2	0.503	13.60	0.39														sec	
D6-501-3.1	41	131	99	0.78	283.6	2.3	0.384	3.8	0.396	13.43	0.51														sec	
D6-501-9.1	24	536	878	1.69	381.7	1.3	0.248	3.8	1.21	12.76	0.25														osc	
D6-501-11.1	61	173	212	1.27	207.3	1.7	0.547	2.6	0.715	12.28	0.58														osc	
D6-501-12.1	42	266	196	0.76	291.1	1.6	0.395	2.6	0.785	12.80	0.35														sec	
KR03-01 D6-1205 (gabbro, stderr = 0.18 %)																									12.94±0.14	0.74
D6-1205-1.1	0.33	277	134	0.50	494.5	1.0	0.0489	3.7	0.481	12.98	0.13	(n = 8)														(n = 8)
D6-1205-2.1	2.6	18	7	0.42	500.7	3.8	0.0667	20	0.0302	12.53	0.52														sec	
D6-1205-3.1	0.92	147	69	0.48	508.9	1.3	0.0536	4.8	0.247	12.54	0.16														sec	
D6-1205-4.1	3.0	52	27	0.53	483.9	2.0	0.0699	7.5	0.0922	12.91	0.28														sec	
D6-1205-5.1	1.7	54	23	0.45	491.2	2.0	0.0597	9.5	0.0953	12.89	0.28														sec	
D6-1205-6.1	0.94	215	148	0.71	493.3	1.1	0.0537	4.0	0.375	12.93	0.15														sec	
D6-1205-7.1	0.47	315	263	0.86	501.3	0.9	0.0500	3.1	0.541	12.79	0.12														sec	
D6-1205-8.1	2.2	90	39	0.45	485.9	1.6	0.0638	5.5	0.159	12.96	0.21														sec	
KR03-01 D6-1401 (gabbro, stderr = 0.18 %)																									13.02±0.11	0.43
D6-1401-1.1	0.64	356	277	0.80	493.3	0.8	0.0513	2.8	0.620	12.97	0.11	(n = 8)														(n = 8)
D6-1401-2.1	0.67	343	331	1.00	496.8	0.9	0.0516	3.2	0.593	12.88	0.11														osc	
D6-1401-3.1	1.0	53	25	0.48	473.0	2.8	0.0542	8.5	0.0966	13.47	0.39														osc	
D6-1401-4.1	1.2	134	108	0.83	495.2	1.3	0.0561	4.7	0.233	12.84	0.17														osc	
D6-1401-5.1	1.3	98	69	0.72	494.3	1.5	0.0565	5.3	0.171	12.86	0.19														sec	
D6-1401-6.1	0.63	347	274	0.82	495.4	0.8	0.0513	2.7	0.602	12.92	0.11														osc	
D6-1401-7.1	0.43	324	264	0.84	495.7	0.9	0.0497	3.0	0.561	12.94	0.12														sec	
D6-1401-8.1	0.56	235	243	1.07	492.0	1.0	0.0507	3.4	0.410	13.02	0.13														osc	
KR03-01 D6-1402 (gabbro, stderr = 0.18 %)																									12.85±0.25	0.74
D6-1402-1.1	0.80	124	68	0.57	497.6	1.3	0.0526	5.2	0.214	12.84	0.18	(n = 8)														(n = 8)
D6-1402-2.1	4.6	21	17	0.83	511.0	3.4	0.0826	14	0.0359	12.02	0.44														sec	
D6-1402-3.1	7.4	22	14	0.67	459.4	3.1	0.105	9.8	0.0413	12.98	0.44														sec	
D6-1402-4.1	4.3	29	16	0.58	468.0	2.7	0.0803	10	0.0538	13.17	0.38														sec	
D6-1402-5.1	5.5	33	21	0.65	482.1	2.6	0.0900	9.2	0.0596	12.62	0.36														sec	
D6-1402-6.1	2.4	21	13	0.64	486.3	3.3	0.0652	17	0.0369	12.93	0.47														sec	
D6-1402-7.1	3.4	43	27	0.65	498.6	2.3	0.0728	8.9	0.0736	12.48	0.31														sec	
D6-1402-8.1	4.4	15	6	0.44	483.8	4.2	0.0811	20	0.0267	12.72	0.60														sec	
KR03-01 D9-101 (leuc																										

D9-101-10.1	28	213	176	0.85	545.7	2.3	0.274	4.2	0.335	8.55	0.25			541.9	2.4	0.272	4.2	8.64	0.26	osc core
D9-101-10.2	39	144	85	0.61	448.1	2.5	0.372	4.2	0.275	8.72	0.35			445.3	2.6	0.370	4.2	8.81	0.36	osc rim
D9-101-11.1	28	224	158	0.73	543.6	2.2	0.277	4.1	0.353	8.55	0.25			539.7	2.3	0.275	4.1	8.64	0.26	osc core
D9-101-11.2	12	593	291	0.51	637.6	1.5	0.148	3.4	0.799	8.86	0.14			631.8	1.6	0.147	3.4	8.96	0.16	osc rim
D9-101-12.1	16	552	319	0.60	618.8	1.6	0.175	4.7	0.767	8.80	0.17			613.5	1.7	0.174	4.7	8.88	0.18	osc rim

KR03-01 D9-102 (leucocratic rock, stderr = 0.13 %)														8.81±0.22	2.02				8.90±0.22	1.98
D9-102-1.1	63	166	112	0.70	279.5	2.0	0.566	3.0	0.509	8.57	0.51	(n = 11)		278.5	2.0	0.564	3.0	8.66	0.51	osc (n = 11)
D9-102-2.1	59	194	114	0.60	299.2	1.9	0.536	3.8	0.558	8.79	0.55			298.0	1.9	0.534	3.8	8.88	0.56	osc
D9-102-3.1	75	76	59	0.80	177.5	2.3	0.663	3.3	0.369	9.22	0.99			177.1	2.3	0.661	3.3	9.32	1.00	osc
D9-102-4.1	44	280	175	0.65	390.2	1.8	0.409	3.3	0.617	9.28	0.32			388.1	1.9	0.407	3.3	9.36	0.32	osc core
D9-102-4.2	27	578	285	0.51	555.8	1.5	0.269	2.7	0.894	8.47	0.16			551.4	1.6	0.267	2.7	8.57	0.17	osc rim
D9-102-5.1	43	362	362	1.03	430.1	1.6	0.404	2.6	0.723	8.50	0.24			427.9	1.7	0.402	2.6	8.58	0.24	osc
D9-102-6.1	10	2280	1528	0.69	649.3	0.8	0.126	2.5	3.02	8.97	0.08			643.6	0.9	0.125	2.5	9.06	0.09	osc
D9-102-7.1	64	153	100	0.67	299.9	2.1	0.578	3.1	0.437	7.66	0.50			298.7	2.1	0.576	3.1	7.76	0.50	osc
D9-102-8.1	69	98	62	0.66	196.4	2.1	0.618	3.1	0.429	10.13	0.80			195.9	2.1	0.616	3.1	10.22	0.80	osc
D9-102-9.1	53	225	190	0.87	360.4	1.9	0.482	2.9	0.537	8.46	0.35			358.8	1.9	0.480	2.9	8.54	0.35	osc
D9-102-10.1	73	79	56	0.73	199.9	2.3	0.652	3.3	0.340	8.65	0.87			199.4	2.3	0.650	3.3	8.72	0.88	osc

KR03-01 D10-305 (leucocratic rock, stderr = 0.13 %)														8.62±0.14	1.65				8.71±0.15	1.57
D10-305-1.1	16	263	167	0.66	588.4	2.2	0.177	5.7	0.383	9.22	0.24	(n = 14)		583.7	2.3	0.176	5.7	9.31	0.25	sec (n = 14)
D10-305-2.1	16	322	120	0.39	626.9	2.1	0.180	4.4	0.441	8.62	0.20			621.1	2.2	0.178	4.4	8.72	0.22	sec
D10-305-3.1	54	51	26	0.52	300.4	3.6	0.496	5.5	0.147	9.79	0.80			299.1	3.6	0.494	5.5	9.88	0.80	unz
D10-305-4.1	17	283	181	0.66	612.8	3.6	0.187	4.3	0.397	8.73	0.33			607.7	3.7	0.185	4.3	8.82	0.34	sec
D10-305-5.1	11	691	391	0.59	660.6	1.4	0.139	3.5	0.898	8.65	0.13			654.5	1.5	0.138	3.5	8.75	0.14	sec
D10-305-6.1	51	64	45	0.74	404.8	3.6	0.465	7.2	0.135	7.86	0.70			402.6	3.6	0.463	7.2	7.95	0.71	unz
D10-305-7.1	49	57	28	0.50	340.6	3.5	0.453	5.5	0.143	9.61	0.66			338.9	3.5	0.451	5.5	9.71	0.67	osc core
D10-305-7.2	35	124	57	0.48	504.3	2.8	0.338	5.9	0.211	8.26	0.39			500.6	2.9	0.336	5.9	8.37	0.39	osc rim
D10-305-8.1	16	393	294	0.77	656.6	1.7	0.177	4.9	0.514	8.26	0.17			651.0	1.8	0.175	4.9	8.35	0.18	sec
D10-305-9.1	19	247	139	0.58	615.8	2.1	0.206	4.4	0.344	8.43	0.21			610.5	2.2	0.204	4.4	8.54	0.22	sec core
D10-305-9.2	35	133	151	1.17	452.8	2.8	0.338	4.4	0.253	9.21	0.36			450.5	2.8	0.336	4.4	9.28	0.37	sec core
D10-305-10.1	33	133	79	0.61	509.9	2.7	0.321	4.7	0.225	8.44	0.32			506.3	2.8	0.319	4.7	8.53	0.33	sec
D10-305-11.1	55	73	53	0.74	359.7	3.1	0.500	4.9	0.175	8.09	0.59			358.0	3.1	0.498	4.9	8.18	0.59	unz
D10-305-12.1	31	155	107	0.71	510.7	2.4	0.301	4.3	0.261	8.73	0.29			507.2	2.5	0.299	4.3	8.82	0.30	sec

KH07-02 D7-002 session1-2 (gabbro, stderr = 0.46 % : session1; 0.17 % : session2)														12.22±0.15	0.97				12.29±0.15	1.03
D7-002-1.1 (s1)	0.62	266	238	0.92	522.4	2.4	0.0512	8.4	0.438	12.25	0.30	(n = 21)		518.6	2.5	0.				

D14-001-12.1	-	150	169	1.17	478.0	2.6	0.0451	13	0.269	13.49	0.36	12.72±0.45 (n = 15)	1.30	475.5	2.7	0.0449	13	13.57	0.37	osc	12.81±0.46 (n = 15)	1.26
KH07-02 D14-006 (gabbro, stderr = 0.16 %)																						
D14-006-1.1	15	46	33	0.75	420.2	5.4	0.168	12	0.0934	13.04	0.81	417.9	5.4	0.167	12	13.05	0.81	sec				
D14-006-2.1	16	32	22	0.70	421.2	6.7	0.174	16	0.0659	12.91	1.02	418.8	6.7	0.173	16	12.92	1.02	sec				
D14-006-3.1	13	30	19	0.65	477.3	7.5	0.151	20	0.0531	11.77	1.01	474.2	7.5	0.150	20	11.81	1.03	sec				
D14-006-4.1	19	34	24	0.72	537.3	7.5	0.200	18	0.0540	9.73	0.90	533.5	7.5	0.198	18	9.75	0.92	sec				
D14-006-5.1	24	27	19	0.71	413.1	7.3	0.235	15	0.0571	12.00	1.12	410.8	7.3	0.233	15	11.96	1.12	sec				
D14-006-6.1	9.8	27	18	0.67	443.1	7.7	0.124	24	0.0528	13.16	1.14	440.4	7.7	0.123	24	13.20	1.16	sec				
D14-006-7.1	6.9	50	40	0.83	456.9	5.5	0.101	17	0.0940	13.15	0.77	454.2	5.5	0.100	17	13.21	0.79	sec				
D14-006-8.1	8.3	55	46	0.86	463.6	5.5	0.112	19	0.101	12.77	0.79	460.9	5.5	0.111	19	12.82	0.80	sec				
D14-006-9.1	10	50	41	0.86	427.6	5.5	0.128	15	0.100	13.55	0.82	425.3	5.5	0.127	15	13.59	0.84	sec				
D14-006-10.1	9.9	50	38	0.79	426.6	5.4	0.125	15	0.101	13.65	0.81	424.2	5.4	0.124	15	13.69	0.83	sec				
D14-006-11.1	8.6	47	37	0.81	409.7	7.7	0.114	15	0.0981	14.42	1.16	407.5	7.7	0.113	15	14.46	1.17	sec				
D14-006-12.1	6.0	33	26	0.79	447.3	7.2	0.0939	28	0.0640	13.56	1.08	444.7	7.2	0.0934	28	13.62	1.10	sec				
D14-006-13.1	4.3	72	63	0.89	490.3	4.8	0.0801	17	0.127	12.59	0.64	487.3	4.8	0.0796	17	12.66	0.65	sec				
D14-006-14.1	9.9	53	50	0.98	457.2	5.3	0.125	14	0.0991	12.74	0.74	454.7	5.3	0.124	14	12.77	0.75	sec				
D14-006-15.1	17	48	37	0.80	418.6	5.5	0.184	13	0.0985	12.79	0.83	416.3	5.5	0.183	13	12.79	0.85	sec				
KH07-02 D18-002Gb (gabbro, stderr = 0.16 %)																						
D18-002Gb-1.1	0.36	1987	5206	2.71	572.6	0.94	0.0491	3.5	2.98	11.21	0.11	mean age of	571.4	1.0	0.0490	3.5	11.23	0.11	osc	mean age of		
D18-002Gb-1.2	-	681	825	1.25	585.5	2.3	0.0455	6.8	0.999	11.01	0.26	magmatic domains	582.3	2.4	0.0452	6.8	11.08	0.27	mix	magmatic domains		
D18-002Gb-2.1	2.2	374	160	0.44	585.9	2.2	0.0633	7.3	0.548	10.76	0.24	(n = 6)	581.0	2.3	0.0628	7.4	10.85	0.26	mod rim	(n = 6)		
D18-002Gb-3.1	2.5	386	263	0.70	591.5	2.1	0.0661	7.1	0.561	10.62	0.24	10.69±0.27	0.07	587.3	2.2	0.0656	7.2	10.70	0.24	mod rim	10.79±0.29	0.08
D18-002Gb-4.1	1.7	454	637	1.45	595.0	2.0	0.0596	7.0	0.655	10.64	0.22	mean age of	591.6	2.1	0.0593	7.0	10.71	0.23	osc	mean age of		
D18-002Gb-5.1	0.36	2632	3948	1.55	564.9	1.3	0.0491	2.9	4.00	11.36	0.15	modified rims	562.0	1.4	0.0488	2.9	11.42	0.16	osc	modified rims		
D18-002Gb-6.1	4.3	88	101	1.19	570.6	4.6	0.080	17	0.132	10.80	0.53	(analyses: 2.1, 3.1,	567.4	4.6	0.0795	17	10.87	0.54	mod rim	(analyses: 2.1, 3.1,		
D18-002Gb-6.2	1.9	413	179	0.45	566.2	2.1	0.0610	7.1	0.627	11.16	0.24	6.1. 10.1)	561.3	2.2	0.0605	7.2	11.27	0.25	osc rim	6.1. 10.1)		
D18-002Gb-7.1	3.2	332	248	0.77	538.9	2.4	0.0717	7.1	0.530	11.57	0.29		535.2	2.5	0.0712	7.2	11.65	0.30	cru			
D18-002Gb-8.1	0.20	2730	2148	0.81	572.5	0.80	0.0479	2.9	4.10	11.23	0.09		568.3	0.9	0.0475	2.9	11.32	0.10	osc			
D18-002Gb-9.1	1.7	467	155	0.34	590.0	1.9	0.0594	6.7	0.679	10.74	0.21		584.7	2.0	0.0589	6.8	10.84	0.22	mix			
D18-002Gb-10.1	1.5	344	243	0.73	593.5	2.3	0.0579	8.0	0.498	10.69	0.25		588.4	2.4	0.0574	8.1	10.79	0.26	mod rim			
KH07-02 D18-002Gr (leucocratic rock, stderr = 0.16 %)																						
D18-002Gr-1.1	1.4	804	2156	2.77	570.5	1.6	0.0576	5.6	1.21	11.13	0.18	(n = 14/15)	569.5	1.6	0.0575	5.6	11.15	0.19	core	(n = 14/15)		
D18-002Gr-2.1	1.2	626	1061	1.75	580.4	1.9	0.0559	7.8	0.927	10.96	0.22		577.2	2.0	0.0556	7.8	11.03	0.22	sec			
D18-002Gr-3.1	2.5	521	842	1.67	579.9	2.0	0.0661	7.0	0.772	10.83	0.23		577.1	2.1	0.0658	7.0	10.89	0.23	osc			
D18-002Gr-4.1	3.5	339	406	1.23	561.8	2.4	0.0735	8.0	0.519	11.07	0.28		558.6	2.5	0.0731	8.1	11.14	0.29	osc			
D18-002Gr-5.1	0.39	451	698	1.60	583.2	3.3	0.0494	7.8	0.664	11.00	0.36		580.0	3.3	0.0491	7.8	11.07	0.37	sec			
D18-002Gr-6.1	4.2	338	459	1.40	585.4	2.4	0.0796	7.2	0.496	10.54	0.26		581.6	2.5	0.0791	7.2	10.61	0.27	sec			
D18-002Gr-7.1	0.																					

D18-005Gr-1.2 (s3)	0.28	604	744	1.27	593.7	1.4	0.0485	6.5	0.873	10.82	0.16		590.0	1.5	0.0482	6.5	10.89	0.17	sec
D18-005Gr-2.1 (s3)	1.8	162	164	1.05	587.8	2.6	0.0601	9.7	0.237	10.77	0.29		584.0	2.7	0.0597	10	10.84	0.30	osc
D18-005Gr-4.1 (s3)	0.46	92	72	0.81	593.5	3.5	0.0499	17	0.133	10.80	0.40		589.5	3.6	0.0495	17	10.88	0.41	osc
D18-005Gr-5.1 (s3)	-	145	176	1.26	574.6	2.7	0.0447	13	0.217	11.23	0.32		571.5	2.8	0.0444	13	11.30	0.32	osc

KH07-02 D18-015 (leucocratic rock, stderr = 0.46 %)																			
D18-015-1.1	1.4	48	35	0.75	549.2	5.1	0.0570	24	0.0753	11.57	0.62	(n = 9)	545.0	5.2	0.0566	24	11.66	0.63	sec
D18-015-1.2	0.11	28	14	0.52	574.9	7.6	0.0470	44	0.0367	9.89	0.80		645.0	7.6	0.0466	44	9.98	0.81	sec
D18-015-2.1	3.0	107	67	0.65	650.5	3.5	0.0698	12	0.159	10.87	0.40		570.5	3.6	0.0693	12	10.96	0.41	sec
D18-015-3.1	5.3	47	29	0.65	538.1	5.1	0.0880	17	0.0744	11.34	0.62		534.1	5.2	0.0874	17	11.43	0.63	sec
D18-015-4.1	-	59	33	0.59	584.4	4.8	0.0380	30	0.0860	11.14	0.55		579.3	4.9	0.0377	30	11.24	0.57	sec
D18-015-5.1	0.14	118	116	1.01	580.5	3.4	0.0474	15	0.175	11.08	0.39		577.0	3.5	0.0471	15	11.15	0.40	sec
D18-015-6.1	3.5	33	18	0.56	598.9	6.6	0.0740	29	0.0477	10.38	0.75		594.0	6.6	0.0734	29	10.47	0.76	sec
D18-015-7.1	3.3	35	13	0.40	563.3	6.2	0.0720	27	0.0531	11.06	0.75		558.3	6.3	0.0714	27	11.17	0.75	sec
D18-015-8.1	7.5	66	53	0.83	604.2	9.7	0.106	13	0.0942	9.86	0.97		599.4	9.7	0.105	13	9.95	0.98	sec

KH07-02 D18-048 session1-2 (gabbro, stderr = 0.46 % : session1; 0.58 % : session2)																			
D18-048-1.1 (s1)	-	60	44	0.76	617.1	4.9	0.0370	30	0.0831	10.57	0.54	(n = 18)	612.0	5.0	0.0367	30	10.65	0.55	sec
D18-048-2.1 (s1)	1.1	17	12	0.71	522.6	8.7	0.0550	43	0.0282	12.18	1.12		519.4	8.7	0.0546	43	12.27	1.13	unz
D18-048-3.1 (s1)	11	20	14	0.70	649.0	8.7	0.134	26	0.0268	8.82	0.89		643.4	8.7	0.133	26	8.91	0.89	unz
D18-048-4.1 (s1)	6.4	23	20	0.92	555.0	7.5	0.0970	27	0.0352	10.86	0.90		551.2	7.5	0.0963	27	10.94	0.91	sec
D18-048-5.1 (s1)	0.0	16	10	0.62	683.1	11	0.0460	57	0.0202	9.43	1.08		676.6	11.0	0.0456	58	9.53	1.10	sec
D18-048-6.1 (s1)	9.7	18	11	0.62	525.5	8.7	0.123	29	0.0291	11.07	1.11		522.2	8.7	0.122	29	11.15	1.12	sec
D18-048-7.1 (s1)	1.0	32	31	0.98	567.1	6.6	0.0540	34	0.0487	11.24	0.79		563.1	6.6	0.0536	34	11.33	0.80	sec
D18-048-8.1 (s1)	7.3	37	19	0.52	517.5	5.6	0.104	17	0.0617	11.54	0.70		513.2	5.7	0.103	17	11.65	0.72	sec
D18-048-9.1 (s1)	8.9	24	17	0.73	595.7	7.4	0.117	25	0.0352	9.85	0.83		591.3	7.4	0.116	25	9.93	0.84	sec
D18-048-1.1 (s2)	19	16	10	0.64	439.9	9.9	0.193	24	0.0303	11.93	1.46		437.3	9.9	0.191	24	12.02	1.46	sec
D18-048-2.1 (s2)	9.1	18	16	0.95	485.8	5.6	0.118	17	0.0311	12.06	0.76		482.9	5.6	0.117	17	12.14	0.76	unz
D18-048-3.1 (s2)	9.0	19	12	0.64	534.4	5.9	0.118	19	0.0298	10.96	0.73		530.5	5.9	0.117	19	11.06	0.74	unz
D18-048-4.1 (s2)	7.5	21	18	0.91	555.9	5.7	0.106	20	0.0323	10.72	0.69		552.1	5.7	0.105	20	10.80	0.70	sec
D18-048-5.1 (s2)	11	15	9	0.64	570.1	7.0	0.130	23	0.0223	10.10	0.82		565.7	7.0	0.129	23	10.19	0.83	sec
D18-048-6.1 (s2)	13	16	10	0.63	566.7	6.6	0.145	19	0.0241	9.94	0.77		562.3	6.6	0.144	19	10.04	0.78	sec
D18-048-7.1 (s2)	4.0	39	40	1.05	578.5	4.1	0.0780	16	0.0582	10.69	0.47		574.6	4.2	0.0775	16	10.77	0.48	sec
D18-048-8.1 (s2)	5.9	26	13	0.52	570.4	5.0	0.0929	18	0.0395	10.63	0.58		565.8	5.1	0.0921	18	10.72	0.59	sec
D18-048-9.1 (s2)	6.8	29	20	0.72	622.1	5.1	0.100	17	0.0396	9.65	0.54		617.0	5.2	0.0993	17	9.74	0.55	sec

KH07-02 D25-201 (leucocratic rock, stderr = 0.46 %)																			
D25-201-1.1	7.4	44	25	0.59	650.7	5.7	0.104	17	0.0584	9.17	0.57	(n = 10)	645.1	5.8	0.103	17	9.27	0.58	sec
D25-201-2.1	4.5	63	39	0.															

Table DR2. Sample mineralogy and dredge locations from cruises KR03-01 and KH07-02.

Cruise	Dredge Site	Dredge Location (WGS84)	Depth (mbsl)	Sample Name	Rock Type	Microstructure	Mineralogy	$^{206}\text{Pb}/^{238}\text{U}$ age (this study)
KR03-01	D6	15°34.56'N 138°51.57'E	5024 - 3855	D6-500	oxide-gabbro (medium-grained type of Harigane et al., 2008)	mylonite	Pl, Cpx, Amp (brown Hb and green Hb), Ilm, Mt, Ap, Zr, Chl	12.82 ± 0.34 Ma
				D6-501	amphibolite/metagabbro (fine-grained type/ultramylonite of Harigane et al., 2008)	ultramylonite	Pl, Amp (brown Hb and green Hb), Ilm, Mt, Ap, Zr, Chl	13.11 ± 0.32 Ma
				D6-1205	amphibolite/metagabbro	weakly deformed	Pl, Amp (brown Hb and green Hb), Ilm, Mt, Zr, Chl	12.94 ± 0.14 Ma
				D6-1401	diorite	undeformed	Pl, Cpx, Opx, Amp (brown Hb), Ilm, Zr	13.02 ± 0.11 Ma
				D6-1402	diorite	undeformed	Pl, Cpx, Opx, Amp (brown Hb), Ilm, Zr	12.85 ± 0.25 Ma
KR03-01	D9	16°26.49'N 139°12.08'E	4765 - 4114	D9-101	granodiorite	weakly deformed	Pl, K-ffsp, Amp, Qtz, Bt, Zr, Mt	8.81 ± 0.14 Ma
				D9-102	granodiorite	weakly deformed	Pl, K-ffsp, Amp, Qtz, Bt, Zr, Mt	8.90 ± 0.22 Ma
KR03-01	D10	16°26.34'N 139°15.55'E	3840 - 3438	D10-305	trondhjemite	undeformed	Pl, Amp, Qtz, Mt, Zr	8.71 ± 0.15 Ma
KH07-02	D7	15°44.21'N 139°09.73'E	5185 - 4914	D7-002	amphibolite/metagabbro	undeformed	Pl, Amp (brown Hb and green Hb), Ilm, Zr	12.29 ± 0.15 Ma
KH07-02	D14	15°18.51'N 139°11.81'E	5858 - 5236	D14-001	amphibolite/metagabbro	undeformed	Pl, Amp (brown Hb and green Hb), Ilm, Mt, Zr, Chl	13.35 ± 0.25 Ma
				D14-006	oxide-gabbro	undeformed	Pl, Cpx, Amp (brown Hb and green Hb), Ilm, Mt, Zr, Chl	12.81 ± 0.46 Ma
				D18-002Gb	oxide-gabbroic portion of sample D18-002	mylonite	Pl, Cpx, Amp (brown Hb and green Hb), Ilm, Zr, Chl	11.27 ± 0.13 Ma
KH07-02	D18	16°04.27'N 139°00.51'E	4999 - 4441	D18-002Gr	feldspathic vein in sample D18-002	undeformed	Pl, Amp (brown Hb and green Hb), Zr	11.11 ± 0.13 Ma
				D18-005Gr	feldspathic vein in sample D18-005	undeformed	Pl, Zr	11.03 ± 0.38 Ma
				D18-015	trondhjemite	porphyroclastic texture	Pl, Amp (brown Hb and green Hb), Ilm, Zr	11.03 ± 0.40 Ma
				D18-048	oxide-gabbro	foliated	Pl, Cpx, Amp (brown Hb and green Hb), Ilm, Zr	10.69 ± 0.35 Ma
KH07-02	D25	16°24.29'N 139°14.17'E	4003 - 3702	D25-201	trondhjemite	foliated	Pl, Amp (brown Hb), Zr	9.34 ± 0.38 Ma

Cpx, clinopyroxene; Opx, orthopyroxene; Amp, amphibole; Hb, hornblende; Pl, plagioclase; K-ffsp, K-feldspar; Qtz, quartz; Bt, biotite; Ilm, ilmenite; Mt, magnetite; Ap, apatite; Zr, zircon; Chl, chlorite. Detailed petrography for D6-500 and D6-501 is presented in Harigane et al. (2008).